

Research Article

¹Department of Anatomy & Cell Biology, McGill University, Montreal, QC, Canada

Keywords

Eukaryotic Initiation Factor 4E, RNA interference, Knockdown, Knockout, Co-immunoprecipitation

Abbreviations

Eukaryotic Initiation Factor 4E	eIF4E
Eukaryotic Initiation Factor 4G	eIF4G
Eukaryotic Initiation Factor 4A	eIF4A
eIF4E Homologous Protein	4EHP
Upstream Activation Sequence	UAS
RNA interference	RNAi
Germline stem cell	GSC
Cyst stem cell	CySC
Individualization complex	IC
Knockdown	KD
Knockout	KO
Co-immunoprecipitation	Co-IP
Tris-buffered saline	TBS
Phosphate-buffered saline	PBS
Sodium dodecyl sulfate polyacrylamide gel electrophoresis	SDS PAGE

Email Correspondence

liang1712@gmail.com

Liang Chen¹

Loss-of-Function Analysis Elucidates Essential Roles of eIF4E Isoforms in *Drosophila* Spermatogenesis

Abstract

Background: Through transcriptional and post-transcriptional regulation, eukaryotic cells can control gene expression to moderate vital cell processes and induce morphological changes. In developmental biology, translation initiation is emerging as a key player in gene expression regulation. Translation initiation begins when eukaryotic initiation factor 4E (eIF4E) binds the 5' mRNA cap to recruit other initiation factors. Eight eIF4E isoforms are present in *Drosophila melanogaster*. The canonical eIF4E-1 is involved in the translation of all genes and is a common target for translational regulation mechanisms. The activity of testis-specific eIF4Es in *Drosophila* are largely unclear, but recent evidence on eIF4E-3 suggests that the other isoforms may also possess distinct, essential functions in spermatogenesis.

Methods: Here we provide protein localization data and loss-of-function analysis to characterize eIF4E-4, eIF4E-5, and eIF4E-7.

Results: Single KD showed few phenotypes, while eIF4E-4/eIF4E-5 double knockdown males had severe defects in spermatogenesis. In eIF4E-5/eIF4E-7 double knockdowns, mutations manifested in multiple stages of severity.

Conclusions: The unique expression patterns and differential mutant phenotypes observed suggest that the testis-specific isoforms contain varying levels of functional redundancy. eIF4E-4 and eIF4E-5, which share close homology, appear to have overlapping roles in regulating germ cell division during early spermatogenesis. However, during spermatid individualization they seem to assume different functions. eIF4E-7 also appears to be involved in germ cell differentiation, but most likely in a separate mechanism due to the inability of other isoforms to compensate for its knockdown.

Introduction

At the crux of many critical cellular processes is the formation, maintenance, and termination of protein localization patterns. With increasing knowledge on gene expression, post-transcriptional regulation is growing as a frontier in developmental biology. This is highlighted by the fact that while mRNA levels can remain stable, the rate of protein synthesis can vary drastically to affect gene expression. (1) Amongst post-transcriptional processes, eukaryotic initiation factor 4E appears to be a central target for regulation. Canonical translation initiation begins when the mRNA is bound at the 5' methylated cap by eukaryotic initiation factor 4E (eIF4E). (2) eIF4E then interacts with eIF4A and eIF4G to form the eIF4F complex, which binds other factors and eventually recruits the ribosome to the bound mRNA (Fig. 1A). (3) As a characterized proto-oncogene, eIF4E is the limiting factor to translation initiation (4) —exogenously increasing eIF4E protein levels will induce cells into an oncogenic state. (2) *Drosophila melanogaster* has eight eIF4E isoforms, and eIF4E-3, 4, 5, 7 are testis-specific (Fig. 1B). (5) All isoforms have been shown to have 5' cap binding at unequal affinities (Fig. 1C). (6) eIF4E-1 is the ubiquitous 5' cap binding protein involved in broad translation of all genes. eIF4E-3 is essential for meiosis during spermatogenesis, with knockouts (KO) forming multi-nucleated spermatocytes and sterile males. (7) Research on eIF4E homologous protein (4EHP) has revealed that it represses translation by sequestering mRNA from eIF4E-1 and preventing eIF4F formation. (8) The function of the other isotypes are largely unknown with only limited information about localization patterns.

The unique developmental properties of the *Drosophila* male germline make it an excellent model to investigate translational machinery. During post-meiotic stages, transcription is virtually non-existent due to the pro-

gressive condensation of germ cell chromatin. (9) Therefore, virtually all de novo protein production during spermatid morphogenesis is a result of translational control. Spermatogenesis begins in the apical tip of the testis and ends at the distal end (Fig. 2A). Somatic cyst stem cells (CySC) and germ-line stem cells (GSC) asymmetrically divide to produce a single spermatogonium that differentiates and undergoes four incomplete mitotic divisions to form 16 interconnected spermatocytes (Fig. 2B). (10) After growing and accumulating gene products to prepare for the oncoming transcriptional arrest, spermatocytes divide meiotically to yield 64 interconnected spermatids that enter spermiogenesis and execute synchronous morphological changes: organelle remodeling, chromatin condensation, cell polarization, elongation, waste bag formation, and individualization. (11) Towards late spermatogenesis, an individualization complex (IC) develops to push excess cytosolic material away from spermatid heads into visible waste bags at the tail terminus (Fig. 2C). (12) When spermiogenesis completes, sperm coil at the terminal epithelium and eject from the testis into seminal vesicles for storage. (13) The entire process takes 10 days, with spermiogenesis taking 5 days.

Here, we provide evidence implicating the vital roles of eIF4E-4, eIF4E-5, and eIF4E-7 in spermatogenesis. Mutants generated from gene-specific knockdowns reveal both unique and redundant functions between isoforms. With their 5' mRNA cap binding ability, eIF4E isotypes are likely able to selectively target populations of mRNAs for translation or repression. Preferential mRNA binding could dictate gene expression throughout the testis and especially during post-meiotic stages—when germ cells no longer produce new mRNA. We hypothesize that eIF4E-5 and eIF4E-7 are essential for male germ cell development, while eIF4E-4 shares functional redundancies with eIF4E-5.

Materials & Methods

Fly Stocks

Flies were raised in glass vials of standard medium as formulated by Bloomington Drosophila Stock Center (BDSC). Stocks were kept in 22°C and flies were crossed in 25°C. Flies were anesthetized and handled on CO₂ pads under a dissecting microscope. Oregon-R flies were used as wild-type controls. To induce gene knockdown, the UAS-GAL4 system was used. (14) Transgenic UAS fly lines express long hairpin RNAi under the control of an upstream activation sequence (UAS). These hairpin constructs are only transcribed when activated by exogenous GAL4 transcription factor, and these are present downstream of endogenous promoters in separate transgenic GAL4 driver lines. We crossed UAS-RNAi lines with a GAL4 driver lines to produce progeny with tissue-specific knockdowns (Fig. 3). (15) Both single and double knockdowns were created (Fig. 4, Fig. 5). The following UAS-RNAi lines from Vienna Drosophila Resource Center (VDRC) and the TRiP project (Harvard Medical School) were used: eIF4E-3 (BL# 42804), eIF4E-4 (VDRC#107595), eIF4E-5 (VDRC#102173), eIF4E-7 (VDRC#107958). The Bam-Gal4;VP16 (gift of M. Fuller) driver was used to express UAS constructs in the spermatogonium. Knockdowns were confirmed with western blot analysis (Fig. 6).

Microscopy

Testes were dissected and prepared under live squash (16) and whole mount immunofluorescence protocols. For live squash prep, testes were dissected in testis buffer with 1.1µg/mL Hoescht 33342 (Invitrogen#62249) and then immediately mounted onto slides to image using the Leica DM6000B microscope. Images were taken 10 minutes after initial dissection to ensure samples maintained structural integrity. For immunofluorescence staining, testes were dissected in 0.3% PBS-Triton X-100, fixed in 4% paraformaldehyde for 15 min, permeabilized in 2% PBS-Triton X-100 for 1 hour, blocked in 0.3% PBS-Triton X-100- 1% albumin for 2 hours, and then probed with antibodies. Samples were probed with the following primary antibodies (raised by H. Han): rabbit anti-eIF4E-1 (1:500), rat anti-eIF4E-3 (1:500), rabbit anti-eIF4E-4 (1:400), and rat anti-eIF4E-5 (1:500). Additionally, rabbit anti-eIF4G (1:500), rabbit anti-eIF4G2 (1:200), mouse anti-Orb 4H8 (Developmental Studies Hybridoma Bank, 1:250), rat and rabbit anti-vasa (1:500), mouse anti- α -tubulin (Sigma #T6199, 1:10000), and mouse anti-adducin 1B1 (Developmental Studies Hybridoma Bank, 1:250) were probed as protein markers. The secondary antibodies used were: Goat anti-rabbit, anti-rat and anti-mouse antibodies conjugated with Alexa 488 or Alexa 555 (Life Technologies). DAPI (Invitrogen #D3571) was used at 10 µg/mL to stain DNA, and Alexa 555 phalloidin (Invitrogen#A34055) was used at 10 µg/mL to stain F-actin. Immunostaining sample images were taken using the Leica SP8 point-scanning confocal microscope, and the images were processed with Fiji software.

Western Blot

To create protein lysate, testes were dissected in 0.3% PBS-Triton X-100, promptly flash frozen in liquid nitrogen, and mechanically lysed in lysing buffer containing 8M urea. 12% SDS PAGE was run, and separated proteins were transferred onto Polyvinylidene difluoride (PVDF) membrane. Blots were blocked in 5% milk for 1 hour and probed overnight with primary antibodies: rabbit anti-eIF4E-4 (1:500), rat anti-eIF4E-5 (1:500), and mouse anti- α -tubulin (1:20,000). After washing with 0.1% TBS-Tween 20, blots were probed for 2 hours with secondary antibodies conjugated to horseradish peroxidase. Using luminol and oxidizing reagent, bound secondary antibodies were visualized with x-ray film.

Co-Immunoprecipitation (Co-IP)

Testes (~80) were dissected in PBS, lysed in 1 mL of lysis buffer (20 mM HEPES pH 7.5, 150 mM KCl, 4 mM MgCl₂, 0.1% (v/v) NP-40, 0.5 mM DTT, 1x Halt protease inhibitor) and centrifuged at 13,000 x g for 10 min. 20 µl Protein G Dynabeads (Invitrogen) were incubated with rabbit eIF4E-1 (1:500) and rat eIF4E-5 (1:500) antibodies for 1 hour. The supernatant was then incubated with Dynabeads overnight on a rotator.

Subsequently, the beads were washed with lysis buffer 3 times for 20 min. The beads were then boiled in SDS sample buffer and the supernatant was used for SDS-PAGE analysis. For western blot, the primary antibodies were rabbit anti-eIF4E1 (1:500), rabbit anti-eIF4G2 (1:500), and rabbit anti-eIF4E-1 (1:1000). HRP-conjugated goat anti-rabbit (1:5000) and anti-rat (1:2500) antibodies (GE Healthcare) were used as secondary antibodies.

Results

Endogenous Expression of eIF4E isoforms in Drosophila Testes

Spermatogenesis begins at the apical tip, and germ cells migrate towards the distal end as they develop (Fig. 7). eIF4E-1 is present in the cytoplasm of both somatic cyst cells and germ cells during early spermatogenesis (Fig. 8). The protein, however, is notably absent in later germ cell stages and instead expresses in somatic cyst cells of spermatid bundles. (17) eIF4E-3 expression is restricted to the cytoplasm of primary spermatocytes, secondary spermatocytes, and early elongating spermatids; it is not localized in stem cells, spermatogonia, or mature spermatid bundles (Fig. 8). (7) eIF4E-4 is found in the cytoplasm of germ cells throughout spermatogenesis. It can be seen that in spermatid bundles, eIF4E-4 preferentially concentrates in the IC and individualized portions of the bundle (Fig. 9A). Interconnected spermatid regions have lower signal strength. eIF4E-5 is also expressed in all stages of germ cell development, including elongating spermatids that produce a ribboning pattern along the testis. The protein abundance increases in waste bags of mature spermatid bundles (Fig. 9A). eIF4E-7 expression patterns were not elucidated. To confirm expression patterns of eIF4E isoforms, antibody specificity was confirmed with western blot (Fig. 6) and immunostaining of knockdown testes (Fig. 9B).

Protein Markers of Spermatogenesis

To analyze phenotypes from eIF4E isoform knockdowns, both cell morphology and protein markers of spermatogenesis were observed. The following protein markers were used: actin, tubulin, vasa, orb, adducin, eIF4G, and eIF4G2 (Fig. 10). In wild-type male flies, phalloidin stains the actin in the outer muscular sheath of the testis as well as the actin cones of the IC (Fig. 10A). (18) α -tubulin is ubiquitously found in the testis, and in spermatids it highlights axonemes (Fig. 10B). (11) eIF4G has similar expression patterns as eIF4E-1, and is found in both the somatic cyst cells and germ cells during early stages, while primarily found in the cyst cells of later germ cells (Fig. 10C). (17) eIF4G2 is a germ-line specific protein (17) and is found in all germ cell stages of spermatogenesis; it concentrates in waste bags (Fig. 1D). Orb is found in the waste bags of individualized spermatid bundles (Fig. 10E). Adducin co-localizes with the fusomes of interconnected germ cells and appears as extensive branches amongst germ cell clusters (Fig. 10F). (20) Vasa is a germline specific protein that chiefly localizes in pre-meiotic germ cell stages (Fig. 10G). (21)

Loss-of-function Analysis of eIF4Es

eIF4E-3 KD flies served as a positive control to test the efficacy of KD mutant generation, and wild-type flies were used as the negative control. eIF4E-3 mutants displayed previously reported phenotypes of male-sterility, multi-nucleated spermatocytes, de-localized nuclei in spermatids, and abnormal orb expression (Fig. 11). (17) eIF4E-4 KD males only showed aberrations towards the distal testis, where coiled spermatids accumulated (Fig. 12). eIF4E-5 KD produced tightly coiled sperm, numerous abnormal cystic bulges, and fewer IC that traveled the entire length of the bundle (Fig. 13).

eIF4E-7 KD males with one UAS-RNAi chromosome driven by Bam-Gal4;VP16 did not display any phenotypes, but after aging males for 4 weeks cells in testes began to over-proliferate and fail to develop into mature sperm. In wild type males, cell proliferation slows as stem cells take longer to divide and differentiate. (22) Males with 2 chromosomes of UAS-RNAi and drivers showed visible phenotypes after only 1-2 weeks of aging. Similarly, these testes were filled with small cells and spermatogenesis was arrested (Fig. 14). Adducin staining showed that only rudimentary fusomes formed in these mutants, indicating these cells did not maintain

connections with each other (Fig. 14)

Double Knockdowns

Although single KD showed few phenotypes, eIF4E-4/eIF4E-5 double knockdown males had severe defects in spermatogenesis. After aging for one week, germ cell development ceased and distal testes contained coiled sperm. Normally, wild type testes show dense concentration of nuclei at the apical tip, but in these double knockdown mutants high concentrations of small cells were found throughout testis (Fig. 14). As a result of these abnormalities, testes lacking orb expression in waste bags show no IC complexes, and have abnormal eIF4G-2 and α -tubulin localization (Fig. 15).

In eIF4E-5/eIF4E-7 double knockdowns, mutations manifested in multiple stages of severity. The least affected testes appeared like wild-type with the entire process of spermatogenesis intact. At the onset of mutation, testes began to show signs of abnormal cyst formation, with problems in differentiation and mitotic division appearing. Through vasa and adducin staining, spermatocytes are seen to occupy only a small portion of the testis (Fig. 16). In the most severe cases, testes were filled with small undifferentiated cells. These mutants lacked orb staining in spermatid waste bags, and instead stained coiled sperm at the distal end (Fig. 16).

Discussion

During germline development, many key cellular processes rely on post-transcriptional gene regulation to establish protein gradients and gene expression patterns. Research across several model organisms point towards translation initiation, namely eIF4E cap binding activity, as a critical stage for post-transcriptional regulation. In *Drosophila*, several control mechanisms target eIF4E. Suppressing translation, eIF4E binding proteins (eIF4E-BP) directly latch onto eIF4E to inactivate it. (23) Repressing translation of specific genes, Bicoid (*bcd*) binds to 3'UTR of Caudal mRNA and recruits 4EHP, a cap-binding protein that is unable to initiate translation, to effectively prevent Caudal protein formation. (8) Recently, eIF4E isoform-mediated translation has been implicated as an alternative way to modulate gene expression. It is important to note that eIF4E-3, eIF4E-4, eIF4E-5, and eIF4E-7 have all been reported to bind eIF4G at varying affinities. (6) This suggests that these male germ-line specific proteins are all able to form the eIF4F complex and initiate translation. However, since only one type of 5' mRNA cap is present in *Drosophila*, eIF4E isoforms would require intermediate proteins like *bcd* to selectively repress or promote translation of specific proteins.

Previous characterizations of eIF4E isoforms have shown that evolutionary conservation between these paralogs differs (Fig. 1B). (6) Amongst the isoforms, eIF4E-4 and eIF4E-5 share the greatest homology. When analyzing single KD's of eIF4E-4 and eIF4E-5, few defects were seen. Spermatogenesis proceeded normally in the mutants up until individualization, during which KD's began to induce mutations. Both eIF4E-4 and eIF4E-5 KD cause sperm to coil at the end of spermatogenesis. Coiling, a morphological deformity, indicates that the mutant sperm are defective and blocked from passing into the seminal vesicle. (13) From observing eIF4E-4/eIF4E-5 double KD, we conclude that the two isoforms share functional redundancies. In stark contrast to single KD, the double KD shuts down spermatogenesis, stimulates uncontrolled cell division, and blocks germ cell differentiation. From immunostaining, eIF4E-4 and eIF4E-5 are seen to co-localize in pre-meiotic cell stages (Fig. 8). This co-localization may explain how the isoforms are able to compensate for the absence of the other in early development. In post-meiotic stages, eIF4E-4 primarily localizes in individuated segments of spermatid bundles while eIF4E-5 is present in all portions of the bundle, including the waste bag. Furthermore, the previously reported reduced fertility of eIF4E-5 may also be explained by these expression patterns: while eIF4E-5 would be able to largely compensate for any absent eIF4E-4 due to the fact that it is ubiquitously present in germ cells, eIF4E-4's absence in non-individuated bundles could contribute to greater cell defects.

From KD analysis, eIF4E-7 seems to be mainly involved in pre-meiotic

germ cell development. These mutants contained a surplus of cells varying in size. Wild type testes usually slow down their rate of stem cell replication and differentiation. (22) While this is likely due to increased production of RNAi, protein and RNA quantification methods need to be performed for confirmation. The phenotypes observed in eIF4E-5 and eIF4E-7 double knockdown are severe, but further analysis is required to determine whether the defects present are merely from eIF4E-7 KD or if they are the result of the KD of both proteins. Therefore it is currently unknown whether eIF4E-7 shares functions with eIF4E-5. Observing eIF4E phylogeny would suggest they do not share functions, as eIF4E-7 has low conservation with other eIF4E isoforms and is almost twice as large as the other eIF4Es.

eIF4E itself is known to be a proto-oncogene (24), and reports have shown that exogenously increasing eIF4E cellular levels can transform cells into tumorous cells. (25) The three eIF4E isoforms observed seem to be involved in cell differentiation and proliferation. Because eIF4E is the rate limiting protein in translation initiation, manipulating native concentrations of this protein can have wide effects on cell metabolism and growth. (3) Over-proliferation can be due to malfunctions in spermatogonial differentiation into spermatocytes or from eliminating the stem cell niche of GSC and CySC through some form of retrograde signaling.

To elucidate the separate functions of the male testis-specific isoforms, Co-IP will be optimized to reveal protein interactions and RNA interactions. This will determine if each isoform forms a preinitiation complex and promotes translation. Previous studies in eIF4E interactions were performed in a Yeast two Hybrid screen, which are known to produce false positives when testing protein interaction. Additionally, performing Co-IP followed by RNA sequencing would elucidate whether isoforms have preferences in binding distinct populations of mRNA. Additionally, knockout (KO) flies can be generated to observe if phenotypes worsen. Since these proteins are overwhelmingly localized in the testis, KO lines should have no effect on the other physiological processes within the fly. Some controls also need to be performed to confirm the phenotypes we observed in the KD flies. RT-PCR and western should be performed on both single knockdowns and double knockdowns. eIF4E-7 localization patterns need to be elucidated. The antibodies raised against this protein that we have is non-specific, so new antibodies raised against a separate peptide of the protein should be created to further characterize this protein. Lastly, mutants should be probed with additional sets of protein markers to discover which molecular mechanisms are disrupted.

Conclusion

Based on distinct localization patterns, variable knockdown phenotypes, and documented protein interactions, we conclude that eIF4E isoforms have essential roles in spermatogenesis. eIF4E-4 and eIF4E-5 are functionally redundant in pre-meiotic sperm development, while they contain separate functions in post-meiotic development. eIF4E-7 is distinct from all other testis specific isoforms and is involved in cell differentiation, proliferation, and stem cell niche maintenance. Characterizations of eIF4E-4, eIF4E-5, and eIF4E-7 contributes to the growing collective knowledge on eIF4E isoform function. Their unique localization patterns and distinct, vital roles indicate that the isoforms are key players in post-transcriptional regulation.

References

1. Jackson R, Hellen C, Pestova T. The mechanism of eukaryotic translation initiation and principles of its regulation. *Nature Reviews Molecular Cell Biology*. 2010;11(2):113-127.
2. Mamane Y, Petroulakis E, Rong L, Yoshida K, Ler L, Sonenberg N. eIF4E \hat{a} € from translation to transformation. *Oncogene*. 2004;23(18):3172-3179.
3. Pelletier J, Graff J, Ruggero D, Sonenberg N. Targeting the eIF4F Translation Initiation Complex: A Critical Nexus for Cancer Development. *Cancer Research*. 2015;75(2):250-263.
4. Richter J, Sonenberg N. Regulation of cap-dependent translation by eIF4E inhibitory proteins. *Nature*. 2005;433(7025):477-480.
5. Chintapalli V, Wang J, Dow J. Using FlyAtlas to identify better *Drosophila*

melanogaster models of human disease. *Nature Genetics*. 2007;39(6):715-720.

6. Hernandez G, Altmann M, Sierra J, Urlaub H, Diez del Corral R, Schwartz P et al. Functional analysis of seven genes encoding eight translation initiation factor 4E (eIF4E) isoforms in *Drosophila*. *Mechanisms of Development*. 2005;122(4):529-543.
7. Hernandez G, Han H, Gandin V, Fabian L, Ferreira T, Zuberek J et al. Eukaryotic initiation factor 4E-3 is essential for meiotic chromosome segregation, cytokinesis and male fertility in *Drosophila*. *Development*. 2012;139(17):3211-3220.
8. Cho P, Poulin F, Cho-Park Y, Cho-Park I, Chicoine J, Lasko P et al. A New Paradigm for Translational Control: Inhibition via 5' cap mRNA Tethering by Bicoid and the eIF4E Cognate 4EHP. *Cell*. 2005;121(3):411-423.
9. White-Cooper H, Caporilli S. Transcriptional and post-transcriptional regulation of *Drosophila* germline stem cells and their differentiating progeny. *Adv Exp Med Biol* 786. 2013;:47-61.
10. de Cuevas M, Matunis E. The stem cell niche: lessons from the *Drosophila* testis. *Development*. 2011;138(14):2861-2869.
11. Fabian L, Brill J. *Drosophila* spermiogenesis. *Spermatogenesis*. 2012;2(3):197-212.
12. Sartain C, Wolfner M. The spermatid individualization complex of *Drosophila melanogaster*. *Mol Reprod Dev*. 2012;79(6):367-367.
13. Tokuyasu K, Peacock W, Hardy R. Dynamics of spermiogenesis in *Drosophila melanogaster*. *Zellforsch*. 1972;127(4):492-525.
14. Dietzl G, Chen D, Schnorrer F, Su K, Barinova Y, Fellner M et al. A genome-wide transgenic RNAi library for conditional gene inactivation in *Drosophila*. *Nature*. 2007;448(7150):151-156.
15. del Valle Rodríguez A, Didiano D, Desplan C. Power tools for gene expression and clonal analysis in *Drosophila*. *Nature Methods*. 2011;9(1):47-55.
16. Bonaccorsi S, Giansanti M, Cenci G, Gatti M. Preparation of Live Testis Squashes in *Drosophila*. *Cold Spring Harbor Protocols*. 2011;2011(3):prot5577.
17. Ghosh S, Lasko P. Loss-of-Function Analysis Reveals Distinct Requirements of the Translation Initiation Factors eIF4E, eIF4E-3, eIF4G and eIF4G2 in *Drosophila* Spermatogenesis. *PLoS ONE*. 2015;10(4):e0122519.
18. Noguchi T, Lenartowska M, Rogat A, Frank D, Miller K. Proper Cellular Reorganization during *Drosophila* Spermatid Individualization Depends on Actin Structures Composed of Two Domains, Bundles and Meshwork, That Are Differentially Regulated and Have Different Functions. *Molecular Biology of the Cell*. 2008;19(6):2363-2372.
19. Xu S, Hafer N, Agunwamba B, Schedl P. The CPEB Protein Orb2 Has Multiple Functions during Spermatogenesis in *Drosophila melanogaster*. *PLoS Genetics*. 2012;8(11):e1003079.
20. Grieder N, de Cuevas M, Spradling A. The fusome organizes the microtubule network during oocyte differentiation in *Drosophila*. *Development*. 2000;127(18):4253-4264.
21. Sano H, Nakamura A, Kobayashi S. Identification of a transcriptional regulatory region for germline-specific expression of *vasa* gene in *Drosophila melanogaster*. *Mechanisms of Development*. 2002;112(1-2):129-139.
22. Boyle M, Wong C, Rocha M, Jones D. Decline in Self-Renewal Factors Contributes to Aging of the Stem Cell Niche in the *Drosophila* Testis. *Cell Stem Cell*. 2007;1(4):470-478.
23. Gingras A. Hierarchical phosphorylation of the translation inhibitor 4E-BP1. *Genes Dev*. 2001;15(14):2852-2864.
24. Carroll M, Borden K. The Oncogene eIF4E: Using Biochemical Insights to Target Cancer. *Journal of Interferon & Cytokine Research*. 2013;33(5):227-238.
25. Lazaris-Karatzas A, Sonenberg N. The mRNA 5' cap-binding protein, eIF-4E, cooperates with v-myc or E1A in the transformation of primary rodent fibroblasts. *Molecular and Cellular Biology*. 1992;12(3):1234-1238.

Images

The images referenced in this article are presented here. Note that the images are *not* chronologically ordered. Visit msurj.mcgill.ca for clearer referenced images.

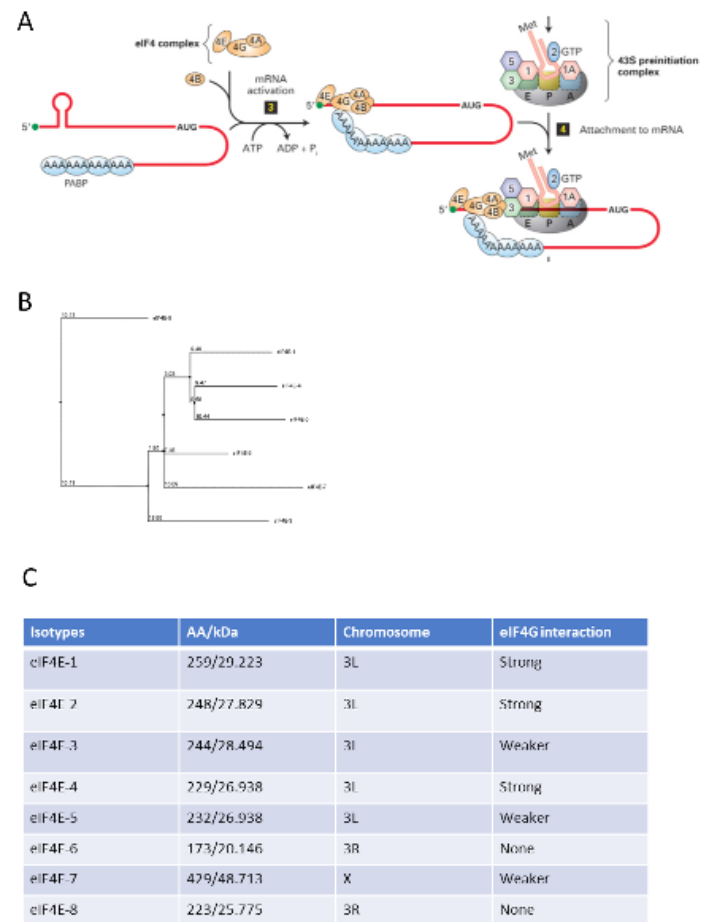


Fig. 1. eIF4E. (A) eIF4E binds to the 5' methyl cap. It then recruits eIF4G that binds eIF4a to form the eIF4F complex and associate with PABP to circularize the mRNA. Afterwards the 43S ribosomal subunit binds to the mRNA. (Molecular cell biology. (Macmillan, 2008)). (B) eIF4E-4 and eIF4E-5 share close homology. (C) eIF4E isoforms are present on the 3rd chromosome. Out of these, eIF4E-6 and eIF4E-8 do not interact with eIF4G.

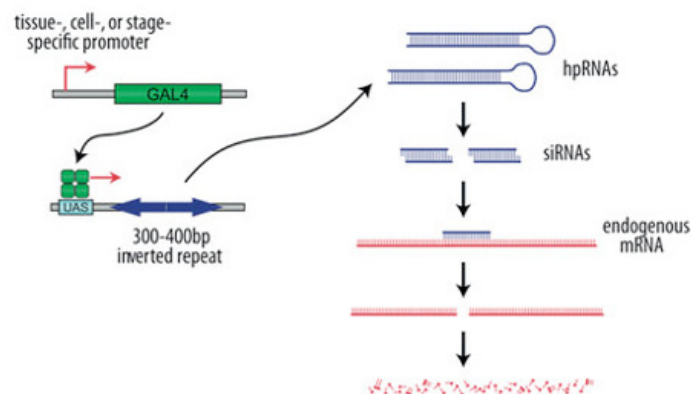


Fig. 3. GAL4/UAS-RNAi System. An endogenous tissue-specific promoter activates GAL4 expression to subsequently bind the UAS promoter and transcribe a ~300 base pair inverted repeat that is complementary to a specific gene. After transcription the RNA forms a hairpin RNA that is processed by Dicer 1 to form small interfering RNA that is recruited and used by RISC to degrade specific mRNAs.

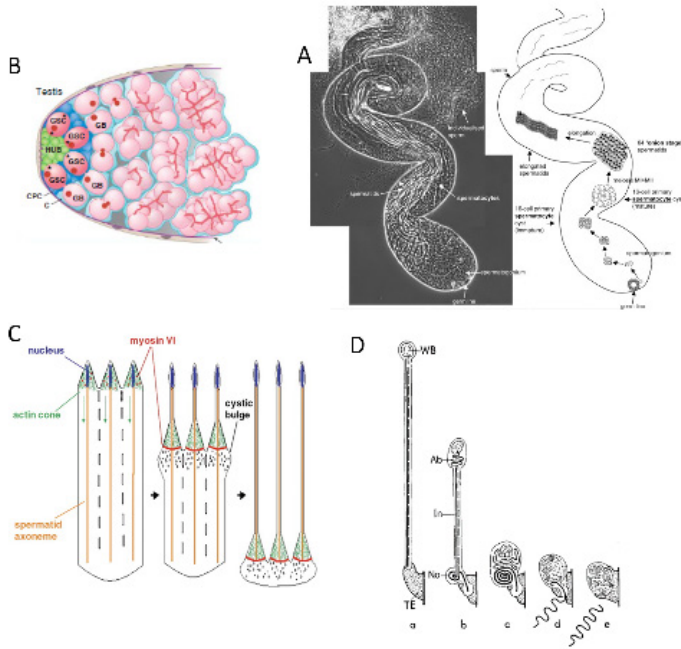


Fig. 2. Spermatogenesis. (A) Spermatogenesis begins at the apical tip where GSC and CySC divide and differentiate. As the cyst develops, it migrates towards the distal end of the testis. Spermatid polarity is maintained with heads facing the distal testis and tails pointing to the apical testis. (B) Fusome develops to interconnect spermatocytes and early spermatids. In spermatogonia, undeveloped fusomes are present as round clusters. (C) Individualization complex (IC) is composed of actin cones and myosin VI that migrates down the spermatid axoneme to individualize sperm and push excess cytosolic content to the tail end, forming waste bags. (D) Only healthy sperm eject from the bundle and eject into the seminal vesicle. Deformed sperm coil into the waste bag, awaiting autophagy.

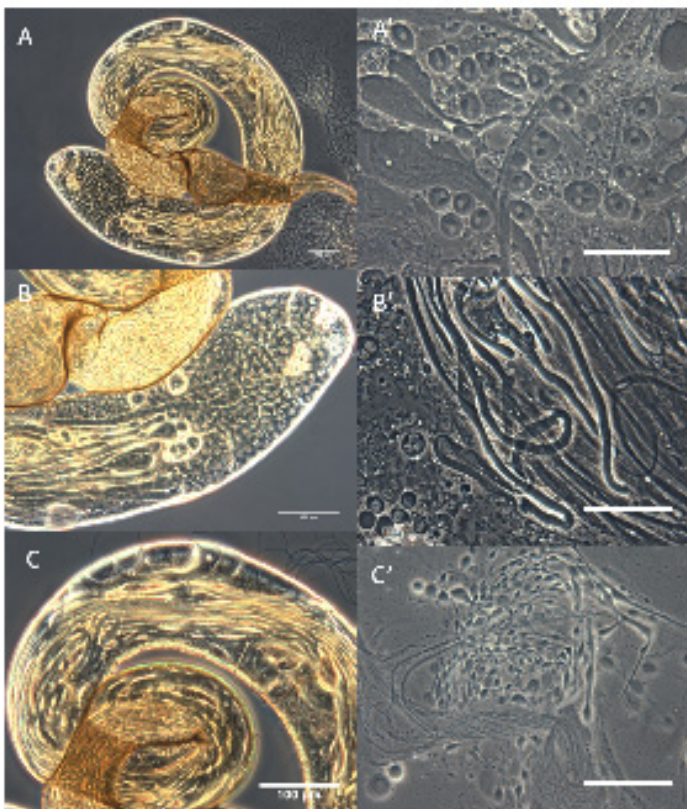


Fig. 7. Wild-type phase contrast testis. (A) Phase contrast image of a wild-type testis. (B) Apical tip can be seen containing CySC, GSC, spermatogonia, and spermatocyte cysts. (C) Distal end shows mature spermatid bundles ready for ejection into the seminal vesicle. (A') Secondary spermatocytes containing dark nebenkern paired with light nuclei. (B') Elongating spermatids that have not yet undergone individualization. (C') Individualized sperm with cystic bulges and waste bags. *Scale bar 100 μ m (n=50)

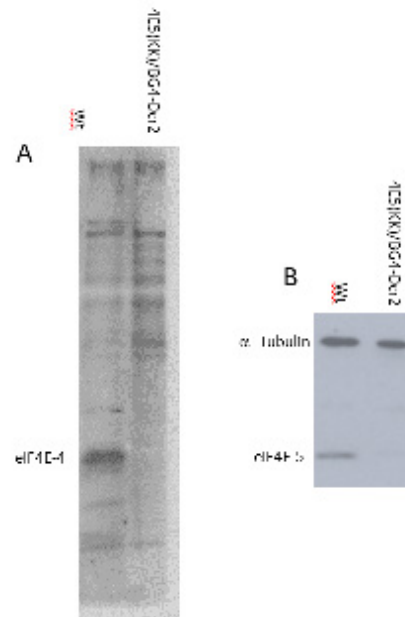


Fig. 6. Knockdown Confirmation. (A) eIF4E-4 is successfully knocked down. The rabbit anti-eIF4E-4 antibody binds non-specifically, and these extraneous bands served as loading controls. (B) eIF4E-5 is knocked down successfully with rat anti-eIF4E-5 antibody. Almost no non-specific bands were bound.

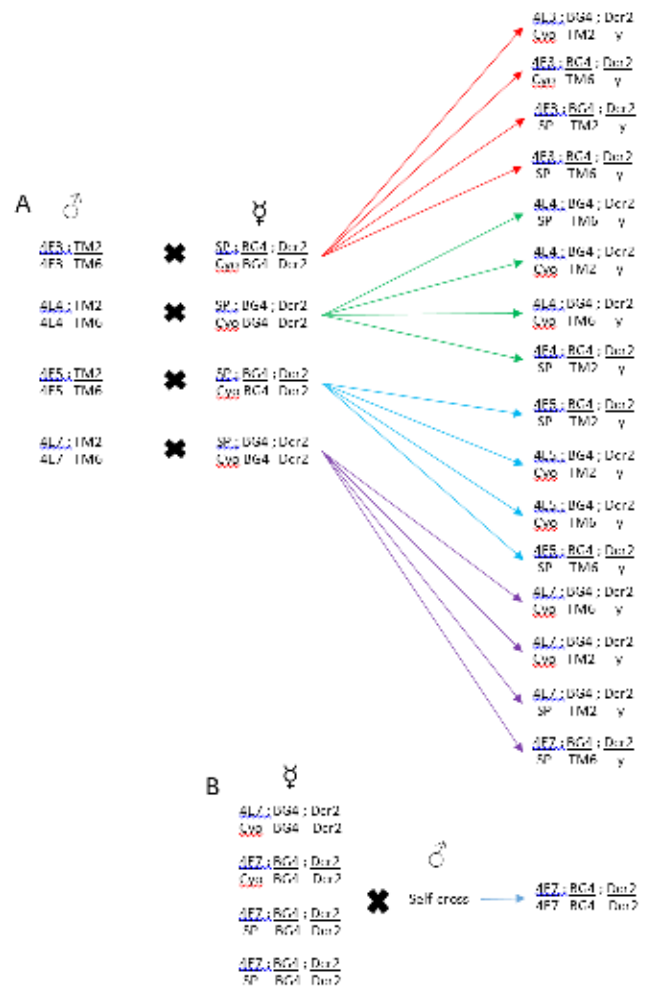


Fig. 4. Single KD Crossing. (A) A single cross was performed to generate single KD crossing. (B) 4E7;BG4;Dcr2 KDs were formed from self-crossing eIF4E-7 single KDs. eIF4E-7 KD males were fertile so crossings were not problematic.

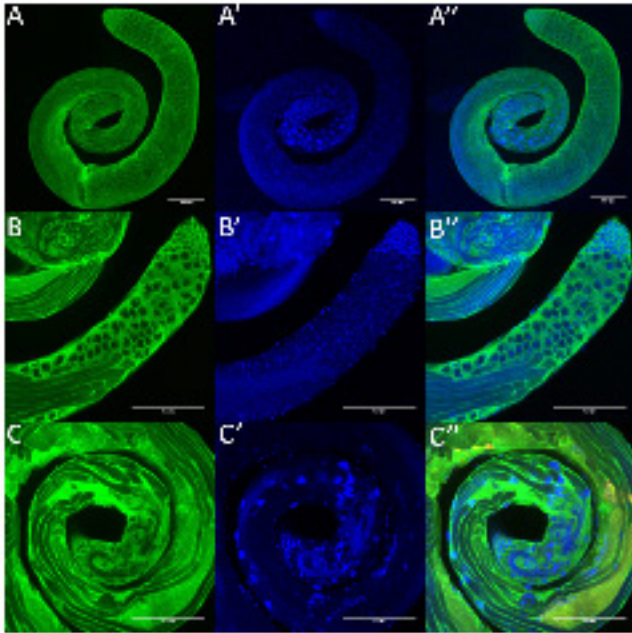


Fig. 8. eIF4E-1 and eIF4E-3 Expression. (A,A') eIF4E-1 stains both somatic cyst cells and germ cells during early spermatogenesis. (B,B') Spermatogonia and spermatocytes contain eIF4E-1 in the cytosol. DAPI staining concentrates at this apical tip. (C,C') eIF4E-1 is only present in somatic cyst cells that surround spermatid bundles during late stage spermatogenesis. DAPI stains clustered nuclei at the heads of spermatids. (D) eIF4E-3 stains germ cells that have not completed meiosis. (E) eIF4E-3 is present in the cytosol of spermatocytes but not in spermatogonia or GSC. (F) eIF4E-3 is seen in early elongating spermatids but becomes absent in subsequent developmental stages.
*Scale bar 100 μ m (n=40)

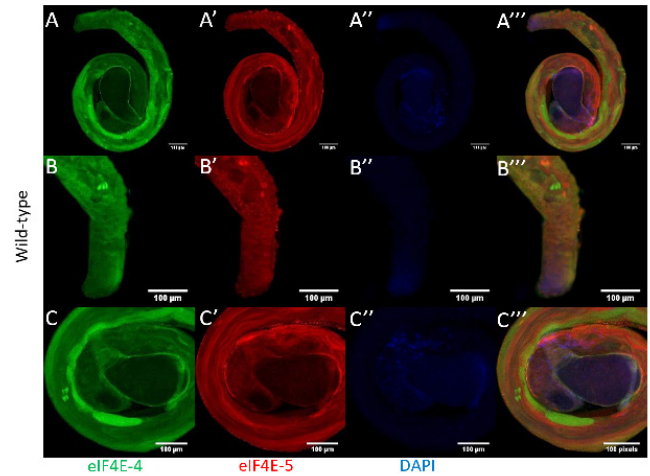


Fig. 9A. eIF4E-4 and eIF4E-5 localization. (A,B,C) eIF4E-4 localizes in germ cells, IC, and post-individualized germ cells. (A',B',C') eIF4E-5 expresses in all germ cells, with increased signal in spermatid bundles and terminal spermatid tails. *Scale bar 100 μ m (n=10)

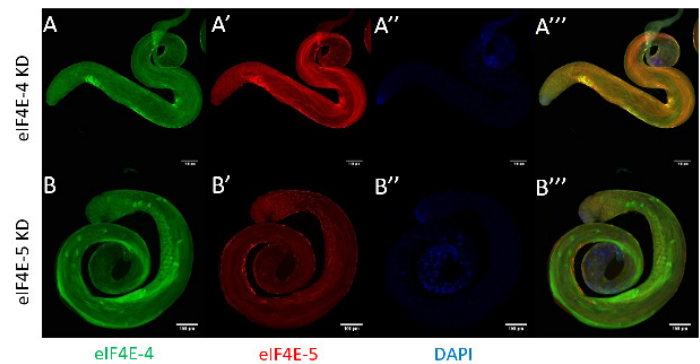


Fig. 9B. eIF4E-4 Antibody confirmation. (A) eIF4E-4 staining is absent in this KD testis. (A') eIF4E-5 staining is unaffected by eIF4E-4 KD. (B) eIF4E-4 staining is unaffected by eIF4E-5 KD, indicating specificity of respective primary antibodies and KDs. (B') eIF4E-5 KD removes eIF4E-5 staining in spermatid bundles. (B'') DAPI in the distal testis shows nuclei remain tightly clustered
*Scale bar 100 μ m (n=10)

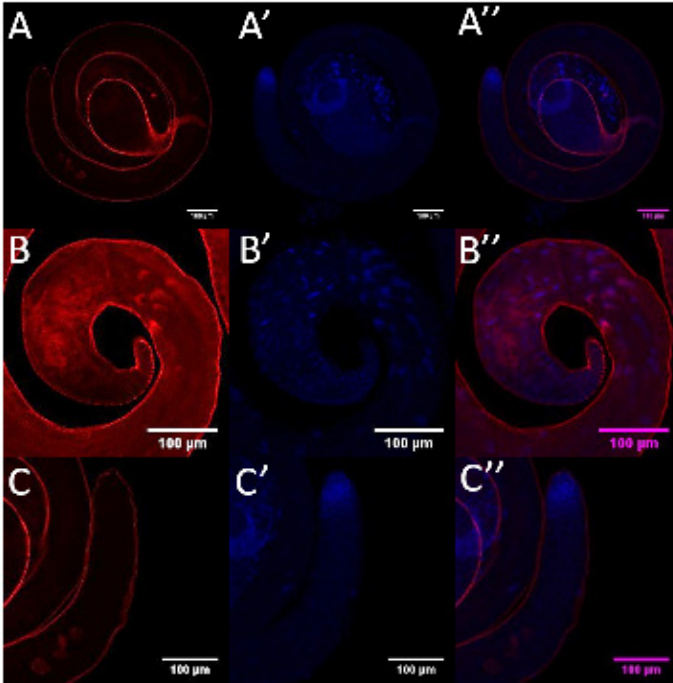


Fig. 10A. Actin localization in testes. The IC is assembled near the distal end (B) and travels down the spermatid towards the tail in the apical end (C)
*Scale bar 100 μm (n=30)

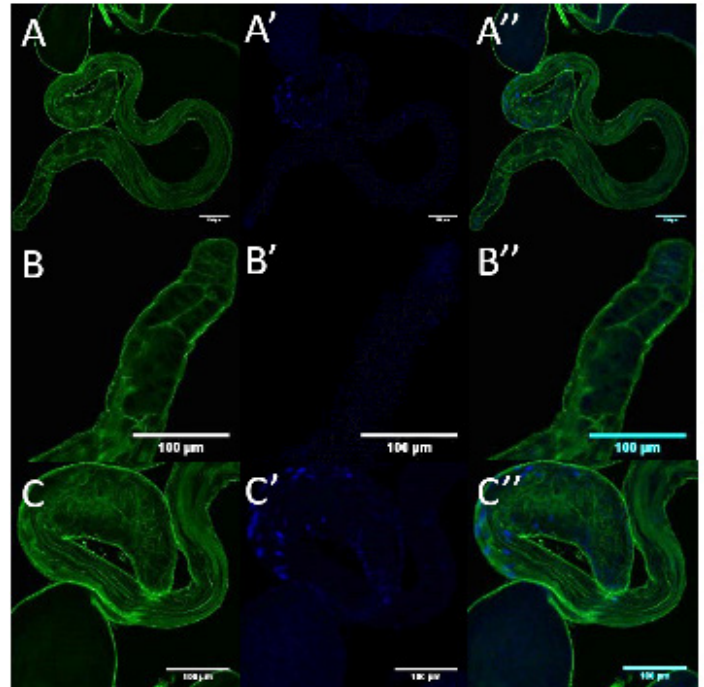


Fig. 10B. A-tubulin localization in testes. a-tubulin is ubiquitously expressed but shows preference for the axoneme (C) and cyst cells (B).
*Scale bar 100 μm (n=30)

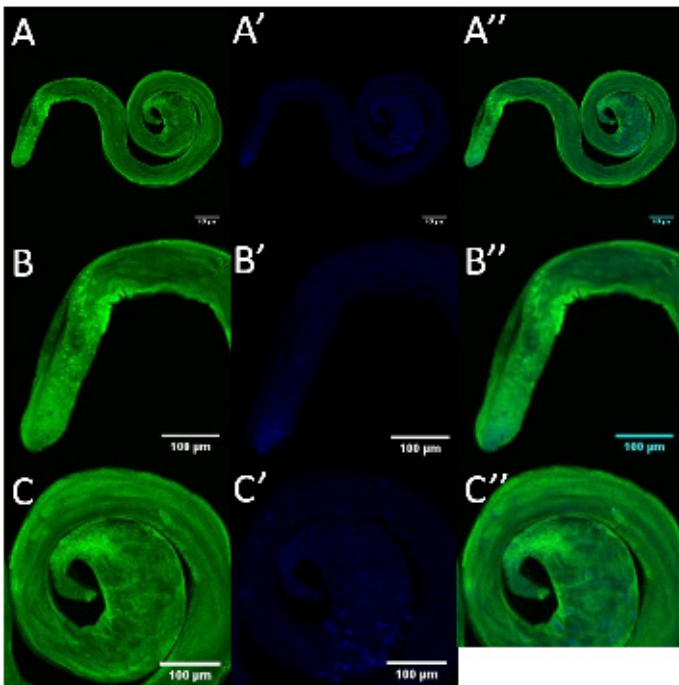


Fig. 10C. eIF4G localization in testes. eIF4G is present in both cyst cells and germ cells at the apical end (B), but only in cyst cells at the distal end (C)
*Scale bar 100 μm (n=30)

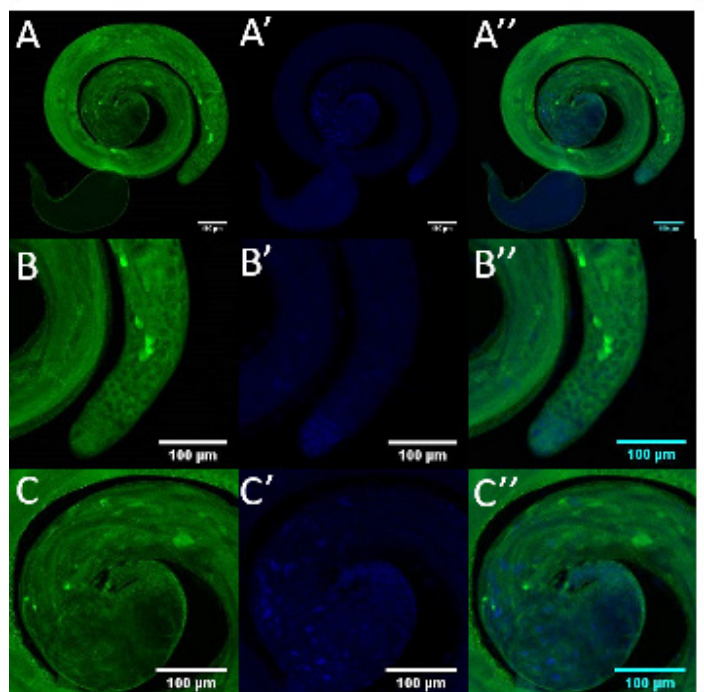


Fig. 10D. eIF4G-2 localization in testes. eIF4G-2 localizes in all germ cells, and shows increased concentration in the terminal ends of spermatid tails (B)
*Scale bar 100 μm (n=30)

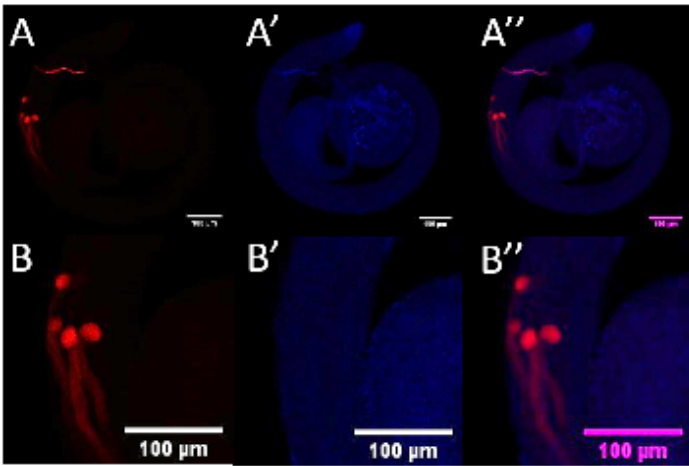


Fig. 10E. Orb localization in testes. Orb exclusively stains the terminal tails of individualized sperm bundles. They collect in the waste bags (B)
*Scale bar 100 μm (n=30)

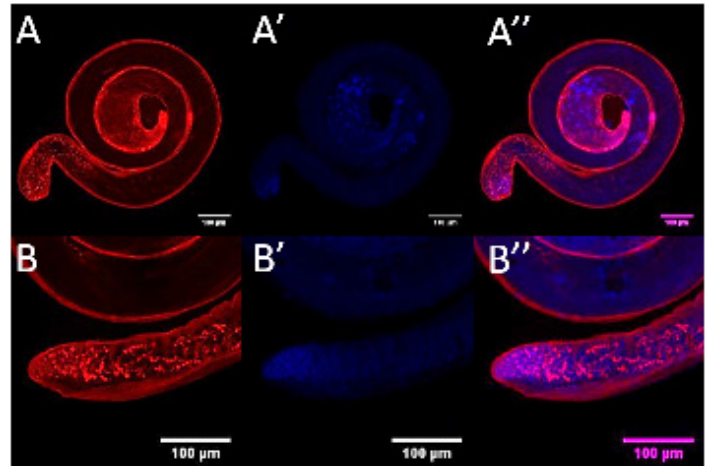


Fig. 10F. Adducin localization in testes. Adducin co-localizes with the fusome, a structure mainly present in pre-meiotic germ cells. This organ maintains interconnections between cell clusters (B) to ensure synchronous development
*Scale bar 100 μm (n=30)

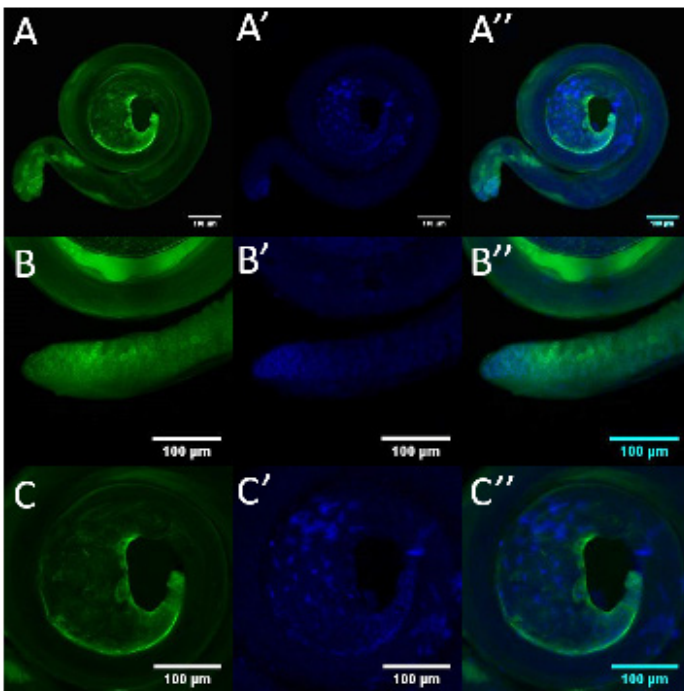


Fig. 10G. Vasa localization in testes. Vasa is a germ-line specific protein that primarily localizes in GSC, spermatogonia, and spermatocytes.
*Scale bar 100 μm (n=30)

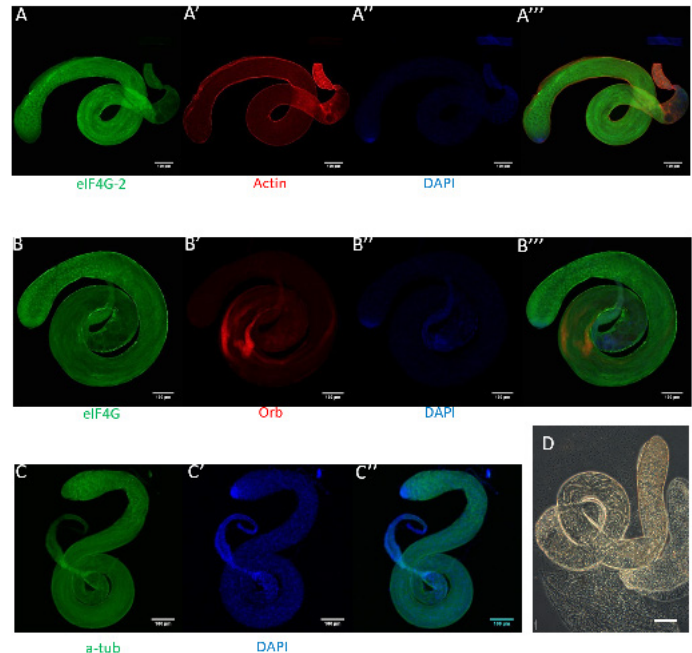


Fig. 11. eIF4E-3 KD. (A) eIF4G-2 distribution in germ cells is normal. (A') Individualization complexes are not present. (A'') Apical DAPI staining remains normal, but subsequent stages show nuclei dispersed along spermatid tails and lack clustered needle nuclei. (B) eIF4G expression is normal. (B') Orb is mislocalized and does not concentrate in waste bags. (C) a-tubulin is ubiquitously expressed and shows axoneme formation. (D) No mature sperm are formed. Spermatocytes contain multiple nuclei per cell.
*Scale bar 100 μm (n=40)

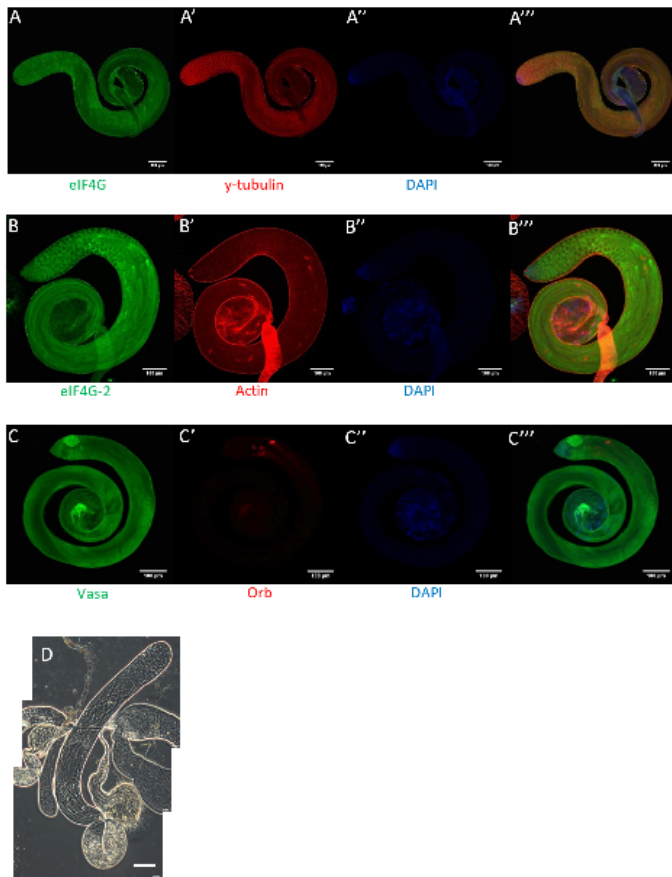


Fig. 12. eIF4E-4 KD. (A,A') eIF4G distribution is undisturbed. (B) eIF4G-2 expression remains the same, with extra signal in terminal spermatid tails. (B') Actin stains IC seen traveling down spermatid bundles. (C) Vasa stains spermatocytes, spermatogonia, and GSC. (C') Orb formation occurs normally in waste bags. (D) Coiled sperm are seen at distal end
*Scale bar 100 μ m (n=40)

Fig. 14. eIF4E-7;BG4;Dcr2 Single KD. (A,B) Vasa continues to stain early germ cell stages, but it can be seen that cell division of these cells occurs with errors. (B) shows that vasa is strikingly absent in these spermatogonia. In (A), cyst formation has ceased and cells no longer form clusters. (A') Adducin shows the fusome is underdeveloped and present throughout the testis, showing that these cells are undifferentiated. (B) shows normal fusome branching, indicating that early germ cells maintain interconnections in some mutants. (C,D) eIF4G-2 appears to have decreased levels in stages before secondary spermatocytes. (C';D') orb staining here is altered. The protein is dispersed and is seen to localize in the middle segment of some spermatids. Distribution is not solely in waste bags. (E) Testis is filled with undifferentiated germ cells. No spermatids are seen
*Scale bar 100 μ m (n=20, 11/20 exhibit phenotypes)

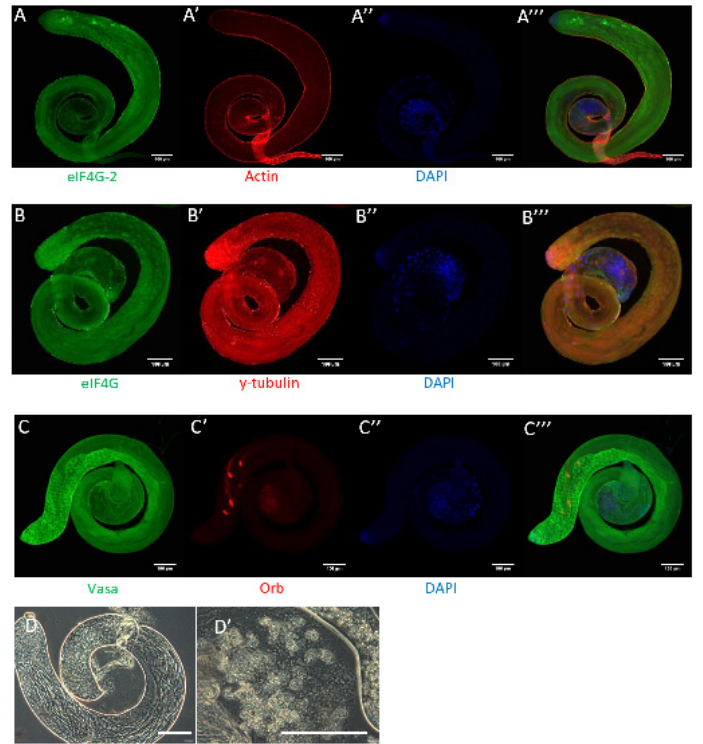
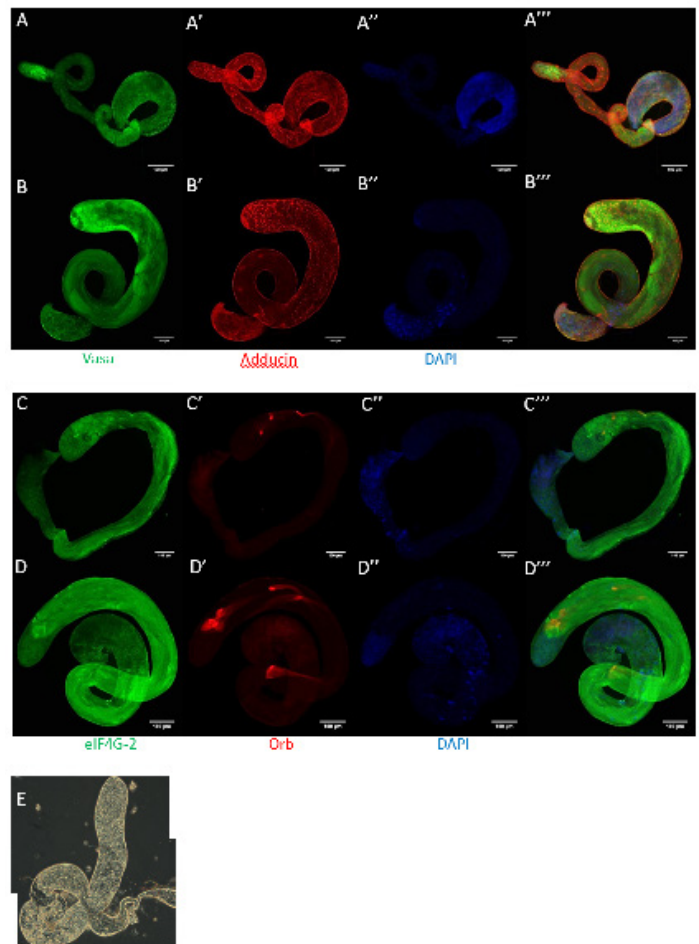


Fig. 13. eIF4E-5 KD. (A) eIF4G-2 expression appears normal. (A') IC are seen in the distal end of the testis but is absent from the apical tip. (B) eIF4G is expressed in germ cells in spermatocytes, but localizes in cyst cells afterwards, as is seen in wildtype (B') γ -tubulin is found ubiquitously in the testis and normally distributed. (C) Vasa is seen primarily staining GSC, spermatogonia, spermatocytes, and early spermatids. (C') Orb formation at the tails of spermatids highlights wastebags. (D) Germ cell development is altered at the distal tip. Abnormal spermatids collect here. (D') Mutant coiled sperm are shown here. They are isolated within cyst cells
*Scale bar 100 μ m (n=50)



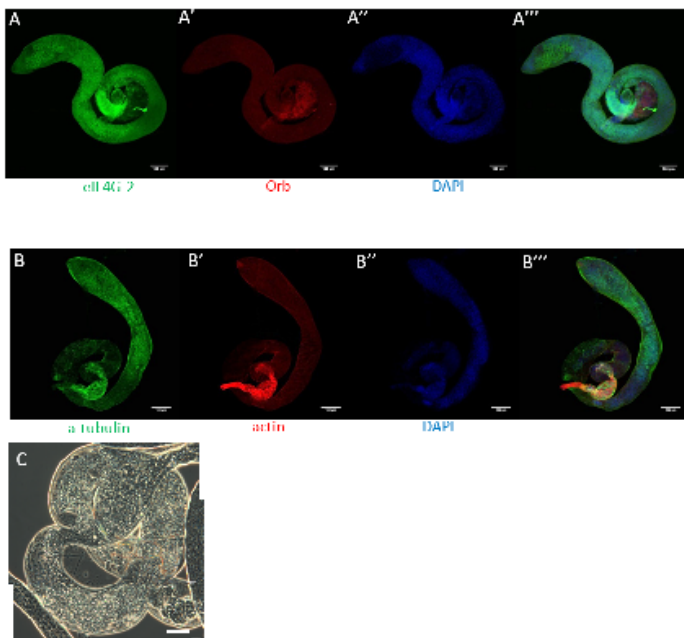


Fig. 15. eIF4E-4/eIF4E-5 Double KD. (A) eIF4G-2 highlight the absence of spermiogenesis. Germ cells do not develop properly and instead remain undifferentiated small cells. eIF4G-2 is absent in the terminus of the testis, where the coiled sperm are located. (A') shows that the small cells fill the entire testis at high concentration. The typically high concentration of DAPI at the apical end is no longer distinguishable. (A') Orb localization is defective and only present in the coiled sperm. No spermatid bundles are developing, so no new waste bags are being formed. (B) a-tubulin shows the lack of axoneme formation. Spermatogenesis has ceased to continue. (B') No IC can be seen. Without spermatids developing, the IC does not assemble. (C) Testis is filled with a mix of undifferentiated cells and coiled sperm. *Scale bar 100 μ m (n=20)

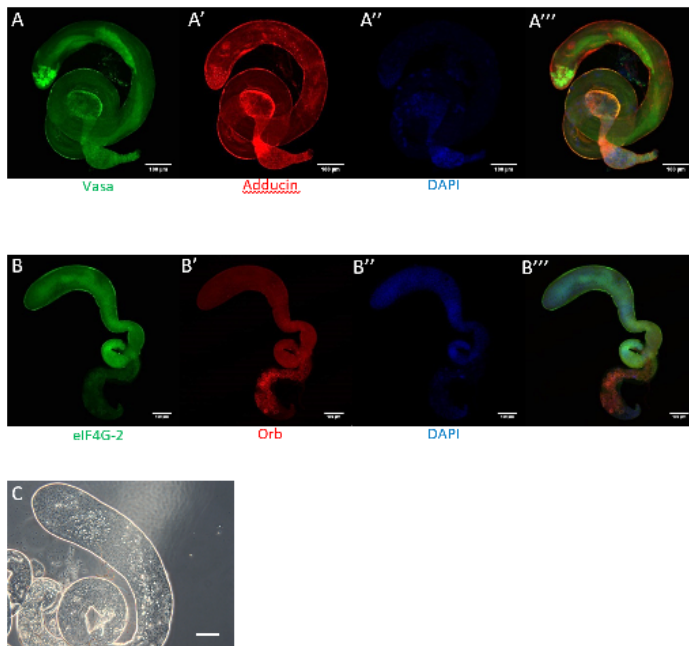


Fig. 16. eIF4E-5/eIF4E-7 Double KD. (A) Vasa only stains a small segment of the testis at the apical end. There is a small number of pre-meiotic germ cells present. (A') Adducin staining supports the data revealed by vasa marker. Fusome branching occurs exclusively in the few spermatocytes left. In comparison to (A'), (B') testis shows more mutations in cell division and differentiation. (B) eIF4G-2 stains the entire testis except for the distal end. The germ cells present in this mutant are approximately the same size throughout (B') Orb shows that this end is filled with coiled sperm. Orb expression is defective due to the absence of spermatid bundles. (C) Early germ cell development is disrupted, with no cyst formation. Coiled sperm are found at distal end. *Scale bar 100 μ m (n=20, 15/20 exhibited phenotypes)

Figure 5. Double KD Crossing. (A) eIF4E-4/eIF4E-5 double knockdown flies were formed here. Three crosses are needed to generate the double knockdown. eIF4E-5 UAS lines were crossed last due to the partial infertility of eIF4E-5 KD. (B) eIF4E-5/eIF4E-7 double knockdown males were generated through this cross

